Kinematic task space scheme for 3dof pneumatic parallel robot in motion control application

Eduardo Izaguirre, Luis Hernández, and Orlando Urquijo

Abstract: The tracking of the wanted position of 3-DOF parallel robot and its orientation in the Cartesian coordinate frame attached to the mobile platform in 3D space (task space) are important in industrial driver simulator's performance. The goal of this work is to implement in a 3DOF parallel industrial robot, a kinematic control scheme in task space coordinates. The inverse kinematics model is used to obtain the desired joint position coordinates from the time-varying trajectory given in task space. The proposed cascade control scheme in task space is based in two loops, the inner loop consisting in a decoupled joint position control and the outer loop which is designed to obtain an appropriate task space positioning. In order to avoid the on-line computation of direct kinematics, an arrangement of inertial sensor and optical encoders are employed to provide the accurate pose measurement of end-effector. The experiments demonstrate the great performance of the cascaded control scheme in motion application.

Keywords: Parallel robot control, Task space control, Motion simulator.

---

1. INTRODUCTION

Parallel robots have received special attention of the systems and control community based on its high force-to-weight ratio and widespread applications [1]. The control schemes for a parallel robot can be divided into two strategies: joint space control [2], and task-space control [3]. The joint space control scheme is based on the information of each actuator length and can be implemented as a decoupled independent single-input single-output control systems for each actuator, with in general, poor compensation of the uncertainties. On the other hand, a task space controller has a potential to provide a better control for the parallel robot under system uncertainties: inertia, modeling error, friction, etc. Nevertheless this type of control scheme needs the direct measurement of system task space state [4] or task space state estimation, normally cumbersome. Task space control schemes have been presented for direct inverse dynamics control, with joint space dynamic model compensation [5] or task space dynamics model compensation, [6], including vision based computed torque in task space control [7]. Many of this schemes have been proved by simulation or in laboratory testbed, but not commonly on industrial motion platform.

Many solutions for task-space based control for both serial and parallel robots can be found. Kim [8] present this control applied to a 6 DOF parallel robot, but require the numerical forward kinematic solution, Qi [9] presents the control based on a combination of fuzzy and sliding mode control, but the system is only tested by simulation. Other solution is based on the dynamic model compensation, but due to the presence of highly nonlinear dynamic coupling, unstructured uncertainties and external disturbance, but the dynamic model of the parallel robot results very complex and will never be exact. Other way is the so-called *kinematic task space control*, where the solution of the numerical forward kinematic and robot dynamic model are avoided, but the tracking problem in the task space is not solved [10].

The goal of this work is to improve the performance of the control system of an industrial 3DOF pneumatic pa-rallel platform, used by SIMPRO company to develop a driver simulator. The solution of the control problem in the joint space of the parallel structure with pneumatic actuators have been obtained by Rubio [11], using a decoupled control based on actuator lineal model around the operational point. But the performance of this scheme is strongly dependent of the precision of the kinematic model and dynamic uncertainties. The solution proposed, the kinematic task space control, is based on the direct measurement of system task space state. The control system considers two loops in cascade, an internal loop solving the robot's joint control (q), and an external loop implementing the task space control (x).

The principal advantage is the simplicity of the control system used, which doesn't need the solution of the forward kinematic and robot dynamic model, very complex tasks in parallel robots.

The good time response, control performance and sta-

Feb, 2014. This work was supported by the Institutional University Cooperation Programme of the VLIR, UCLV and Flemish Universities

E. Izaguirre, L. Hernández, and O. Urquijo are with Universidad Central Marta Abreu de Las Villas, C. Camajuani Km. 5, 54830, Santa Clara, VC, Research Group of Automatic, Robotics and Perception, Cuba (e-mail: { izaguirre, luishs, orlandop}@uclv.edu.cu).

bility of the proposed control system are demonstrated, where experimental results confirm the expected response of the parallel robot in the task space coordinates in motion control application.

The paper is organized as follows: In section 2., the robot description and the kinematic and electro-pneumatic actuators models are presented. Consequently in the section 3. exteroceptive pose measurement is exposed as the practical solution for measure the task space robot's coordinates. The control problem is formulated in the section 4., where the solution of joint decoupled control and robustness analysis is done. The kinematic task space proposed control, is given in section 5. with experimental results described in section 6.. Finally section 7. gives some concluding remarks.

2. KINEMATIC ROBOT DESCRIPTION

As shown in Fig. 1, the robotic system considered consists of a 3DOF parallel manipulator controlled by pneumatic actuators. The parallel robot is produced by SIMPRO for driving simulator purpose, the robot has sensors to measure the joint displacements and the task space states. The basic mathematical description of this system consists of the parallel robot kinematic and dynamic model of the electro-pneumatic actuators.

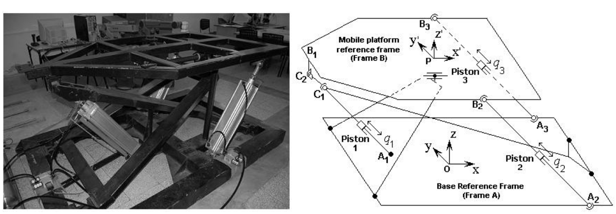

Fig 1: SIMPRO 3DOF pneumatic motion simulator and its RPSU-2SPS kinematic structure

Likewise the serial manipulators, kinematics relations of parallel robots give the relationship between the joints variables $\mathbf{q}$ and the corresponding position (x,y,z) and angular orientation (θ,φ,ψ) of center of mass of mobile platform in cartesian space. For an n-axis parallel structure, the forward kinematic (FK) solution $\mathbf{T}$ could be numerically computed according with the number of joints of kinematic architecture [1]. Generic mathematical representation of forward kinematics could be:

$$\mathbf{x} = \left[\ x\,y\,z\,\theta\ \varphi\ \psi\ \right]^T = f(q_1,q_2,\ldots,q_n) = \mathbf{T} \qquad (1)$$

For parallel robots, the complexity of FK equations increase notably with the numbers of degree of freedom, the solution is non-unique and numerical methods are currently used to obtain the solutions. Unfortunately there is no known algorithm that allows the determination of the current pose of the platform among the set of solutions. Furthermore, the computation times involved in FK algorithms are still too many for use in a real time application [1].

For robot path planning, the inverse kinematic (IK) expression $\mathbf{T^{-1}}$ gives the joint coordinates $\mathbf{q}$ required to reach the specified pose of mobile platform. The mathematical expression of inverse kinematics can be written as:

$$\mathbf{q} = \left[\ q_1\ q_2\ \ldots\ q_n\ \right]^T = g(x,y,z,\theta,\varphi,\psi) = \mathbf{T}^{-1} \qquad (2)$$

Schematic of the 3DOF parallel robot under study is shown in Fig. 1. The system consists of a fixed base connected to a moving platform by three actuated kinematics chains, following the RPSU-2SPS architecture. A base coordinate frame designated as $Oxyz$ frame is fixed at the center of the base with its z-axis pointing vertically upward and the x-axis pointing backwards of the platform. Similarly a moving coordinate frame $Px'y'z'$ is assigned to the center mass of the moving platform, with the z'-axis normal to the mobile platform. By simplicity, the directions of both z and z' axes are pointing in the same unit vector.

The actuators are double effect electro-pneumatic cylinders, whose lineal displacements produce the 3DOF of the robot, consisting in two rotations around the x' and y' axes, represented by roll (θ) and pitch (φ) angles respectively, and linear displacement along the z' axis (elevation), defined by the variable h. So, the moving platform can simulate different sceneries in correspondence with the virtual reality world shown in a LCD display located inside the cabin which is supported by mobile platform.

The vectorial formulation is used to develop the inverse kinematics relations, where the set of equations contains the same number of equations as the unknown variables [1], where the closed vector cycle is constituted between the points A_i and B_i in correspondence with the illustration represented in Fig. 2.

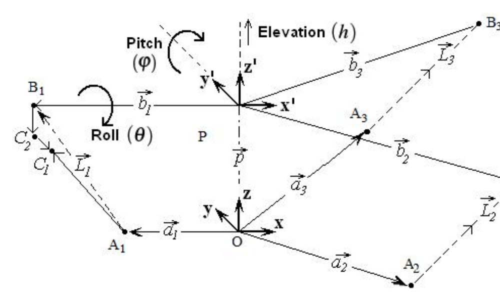

Fig 2: Representation of closed loop vectors of active legs

Establishing the inverse kinematics model is essential for the position control of the robot. Then, for each kinematics chain, a vectorial function can be formulated by expressing the actuated joint coordinates $(\mathbf{q})$ as a function of cartesian coordinates $(\mathbf{x})$ which define the pose of the mobile platform. According to equation (2) the relation

$\mathbf{A}_i\mathbf{B}_i = g(\mathbf{x})$ was found in order to calculate the inverse kinematics model of the robot.

The position vector of the mobile platform with reference to the fixed frame is defined by the vector $\overrightarrow{p} = \overrightarrow{OP}$, that is, the position (elevation) of the platform in cartesian space is defined by z' coordinates of point P. Consequently, the orientation of mobile platform is determined by θ and φ angles.

Using the notation illustrated in Fig. 2, the inverse kinematic expressions can be written from the loop closure equation for each actuated kinematic chain. A complete inverse kinematics study of the 3-DOF parallel mechanism and validation of IK equations can be found in [12], including singularities analysis, where the existence of nonsingular configurations in the robot's workspace are demonstrated.

2.1. Electro-pneumatic actuators model

In order to obtain the dynamic model of a pneumatic cylinders, the influence of the underlap characteristic of the flow servo-valve is considered [11]. Under this conditions, the transfer function of the electro-pneumatic system, position $Y_0(s)$ versus control action $U_0(s)$, is obtained in the operating point of the flow servovalve (3).

$$\frac{Y_0(s)}{U_0(s)} = \frac{b_0}{s\,(s^2 + c_1 s + c_0)} \tag{3}$$

The coefficient b_0 is the gain system, $c_1 = 2\xi\omega_n$ and $c_0 = \omega_n^2$; where ω_n and ξ are respectively the open loop undamped natural frequency and damping ratio of the system.

The linearized version of electro-pneumatic system are developed by dynamic on-line identification following the block diagram shown in Fig. 3. The position's transfer function Y(s) from the valve input voltage U(s) is obtained based on previous works development firstly in 2-DOF pneumatic platform [11], and subsequently extending to 3-DOF motion simulator [13].

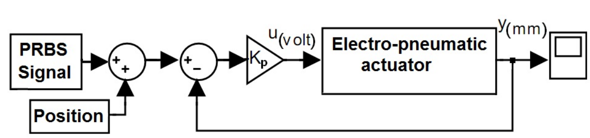

Fig 3: Representation of block diagram for dynamic online identification

The corresponding transfer functions obtained by close loop experimental identification are shown in expressions 4 and 5 for actuator 1 and actuators 2-3 respectively.

$$Actuator\ 1: \quad \frac{Y_1(s)}{U_1(s)} = \frac{246}{s\,(s^2 + 7.73s + 253)} \tag{4}$$

$$Actuators\ 2,3: \quad \frac{Y_{2,3}(s)}{U_{2,3}(s)} = \frac{2008}{s\,(s^2 + 7.28s + 1349)} \tag{5}$$

The kinematic control based on the dynamic model of actuators does not required to computed the inverse dynamic matrices, it is simple and very useful for real-time implementation with low samples period.

3. POSE MEASUREMENT SYSTEM

On line computing of direct kinematics of PKM in real time applications demand high performance of the computer hardware, additionally task space control schemes based on forward kinematics are affected by the numerical estimation errors and the geometrical errors, both typical characteristics of direct kinematics problem of parallel robots applications [14]. Based on the general idea of J. Gao [4] , the combination of exteroceptive sensorial system consisting of optical encoders and inertial measurement unit is proposed to efficiently measured the pose of moving platform [15].

In that case, the vector of cartesian coordinates of the end-effector positioning is measured by the arrangement of exteroceptive sensors as is shown in Fig. 4.

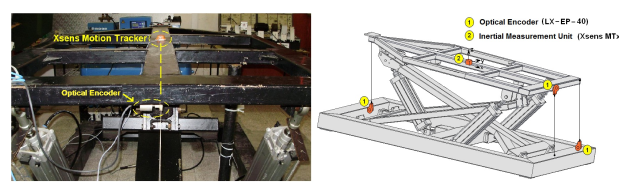

Fig 4: Arrangement of sensors located on the moving platform for measure the end-effector pose

Thanks to the combination of the optical encoders and inertial measurement unit, a fast and accurate end-effector pose measure is available in real time for control purposes.

4. CONTROL PROBLEM

The control problem is formulated as the design of a controller which computes a control signal corresponding to the movement of the robot in such a way that the desired task space position be reaches following wanted performances index.

The control the desired state $\begin{bmatrix} \theta_d & \varphi_d & h_d \end{bmatrix}^T$ is the position of center of mass of mobile platform, so the task state error is then defined as:

$$\tilde{y} = y_d - y = \begin{bmatrix} \tilde{\theta} \\ \tilde{\varphi} \\ \tilde{h} \end{bmatrix} = \begin{bmatrix} \theta_d \\ \varphi_d \\ h_d \end{bmatrix} - \begin{bmatrix} \theta \\ \varphi \\ h \end{bmatrix}$$

which could be calculated at every measurement time and used to move the robot in a direction allowing its decrease. Therefore, the control aims at ensuring that:

$$\lim_{t\to\infty} \tilde{y} = \lim_{t\to\infty} \begin{bmatrix} \tilde{\theta} & \tilde{\varphi} & \tilde{h} \end{bmatrix}^T = 0$$

The assumption for the control problem is that, the control problem is evaluated with initial error $\tilde{\xi}(0)$ and it is sufficiently small and also exists a robot joint configuration $\mathbf{q}_d$ in which the condition $\xi_d = \xi(\mathbf{q}_d)$ is fulfilled.

4.1. Joint control

The electro-pneumatic actuators systems consist of proportional flow valve type MPYE-5-3/8 connected to double-acting pneumatic cylinder FESTO DNC-125-500. The actuator model was obtained by dynamic identification [11], where the bandwidth and magnitude of the pseudo random binary input signal were selected to obtain the adequate excitation of the robotic system. The experimental dynamic identification resulted in the electro-pneumatic systems models described by (4) and (5)

The transfer functions of joints controllers are designed for two conjugated complex poles dominated with $\xi = 0,7$ and ω_n=10 rad/s, where the general proposed closed loop transfer function is:

$$\frac{B_m}{A_m} = \frac{k_p\, b\,(s+k_i)}{(s+p_1)(s+p_2)(s^2+2\xi\,\omega_n\, s+\omega_n^2)} \tag{6}$$

The p_1 and p_2 are two non dominant poles, selecting together with the parameters ω_n and ξ using the pole placement method [11], [12].

The obtaining transfer functions of controllers are describing by (7) and (8) for actuator 1 and actuators 2-3, respectively.

$$\frac{U_1(s)}{E_1(s)} = \frac{265(s^2+7.726s+253)(s+3.03)}{s(s^2+146.7s+6267)} \tag{7}$$

$$\frac{U_{2,3}(s)}{E_{2,3}(s)} = \frac{32(s^2+7.726s+1349)(s+3.03)}{s(s^2+146.7s+6267)} \tag{8}$$

The control system must be designed to provide high speed, low error, and positioning repeatability. An embedded controller provides a control signal to electropneumatic valves, which drives the pneumatic cylinders. This type of pneumatic system is low in cost, and provides adequate dynamic and accuracy performance, in the motion control application.

Then de joint control scheme is implemented following the block diagram shown in Fig. 5

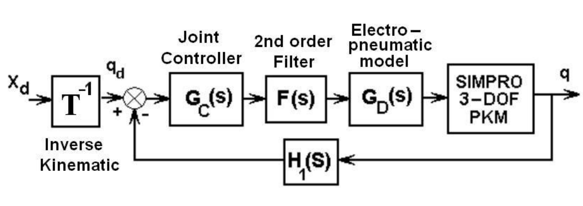

Fig 5: Joint space position control scheme

4.2. Robustness analysis

In order to analyze the robustness against dynamic interactions of the proposed joint control scheme, the amplitude of sensitivity function of the transfer function $Y(s)/U(s)$ is evaluate around the operation frequency of the motion simulator. For robustness analysis the control loop of Fig. 5 can be redraw as is shown in Fig. 6

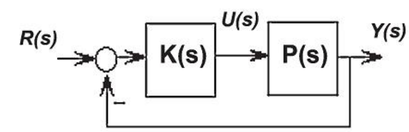

Fig 6: Simplified control scheme for robustness evaluation of closed loop system

The sensitivity function S_P^h is obtained as the relation between the closed loop output variations $h(s)$ respect to the variations of the transfer functions of the plant $P(s)$, and it is calculated by expression (9).

$$S_P^h = \frac{\partial h}{\partial P}\frac{P}{h} = [1+P(s)K(s)]^{-1} \tag{9}$$

where:

$$h(s) = \frac{P(s)K(s)}{1+P(s)K(s)} \tag{10}$$

The Bode magnitude of the output sensitivity respect to the variations of the transfer function of the plant is shown in Fig. 7, where no peaks are observed in the closed loop magnitude. In particular, the magnitude value of -38 db is achieved at operation frequency of robot ($W(j\omega)$=0.82 rad/sec). This is an acceptable attenuation value as a guarantee of robust performance of the system for the practical application of motion simulator.

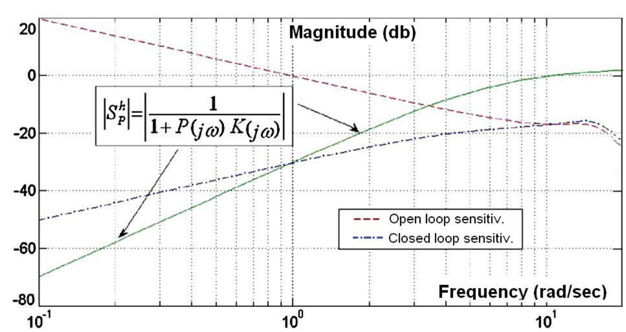

Fig 7: Bode diagram of the loop sensitivity functions

5. KINEMATIC CONTROL SCHEME

A direct knowledge of the desired joint position $\mathbf{q}_d$ is not available. Nevertheless, the desired joints positions can be obtained as a result of the estimated control signal and the solution of the kinematics problem.

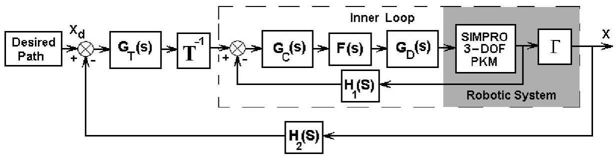

Fig 8: Kinematic task space control scheme

The implemented closed-loop block diagram can be described as shown in Fig. 8. The control system has two loops in cascade, the internal loop solving the robot's joint control, and the external loop implementing a kinematic task space control.

The inner control loop has open control architecture; in this architecture it is possible to implement any type of controller. In such way the dynamic effect of the internal loop could be independent with regard to the external loop, being under the conditions that:

$$\mathbf{q}(t) = \mathbf{q}_d(t) \quad \forall t > 0 \tag{11}$$

Because the dynamics of the inner loop could be represented as one (or two) delay units of the external loop [16], the equation (11) is modified as,

$$\mathbf{q}(k) = \mathbf{q}_d(k-1) \quad \forall k > 0 \tag{12}$$

According to the approximation (12), the following simplified control scheme of Fig. 9 can be considered.

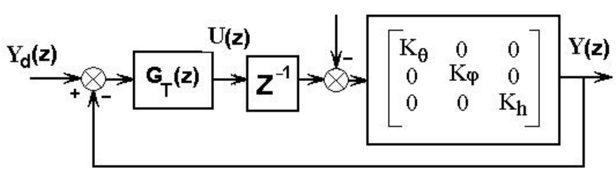

Fig 9: Simplified control scheme

A simple integral controller can be used in this control scheme, where the control law can be given by:

$$G_T = \mathbf{K}_I \int \tilde{\mathbf{y}}(t) \tag{13}$$

Where $\mathbf{K}_I \in \Re^{3\times 3}$ is the symmetric integral matrix:

$$\mathbf{K}_I = \begin{bmatrix} K_{I_1} & 0 & 0 \\ 0 & K_{I_2} & 0 \\ 0 & 0 & K_{I_3} \end{bmatrix} \tag{14}$$

The coordinates increment in the task space can be interpreted as a result of the direct measurement of the center of mass of moving platform pose. Solving the inverse kinematics problem T^{-1} it is possible to obtain $\mathbf{q}_d$.

The task space coordinates are measured by the arrangement of linear sensors [15], representing by the measuring gain matrix $\mathbf{K_M}$ as,

$$\mathbf{K_M} = \begin{bmatrix} K_\theta & 0 & 0 \\ 0 & K_\varphi & 0 \\ 0 & 0 & K_h \end{bmatrix} \tag{15}$$

Taking into account Fig. 8, obtaining the discrete equivalence of the controller of equation (13), according to equations (12) and (14) and taking a sampling period of 60 ms, the following transfer function for the digital controller is derived:

$$G_T(z) = \frac{0.06 K_I}{z-1} \tag{16}$$

Then, considering (16), the closed loop transfer function of the simplified system represented in the Fig. 9, can be written as:

$$\frac{0.06\ \mathbf{K_I}\ \mathbf{K_M}\ z^{-2}}{(1-z^{-1})} [\mathbf{Y_d}(z) - \mathbf{Y}(z)] = \mathbf{Y}(z) \tag{17}$$

It is easy to conclude that the control system is decoupled in each task space coordinate, i.e., the roll, pitch and elevation of mobile platform, where the cartesian coordinates of mobile platform are described by different stable expressions.

For purpose control, the closed loop poles of robot elevation, for example, are selected for the gain $K_h K_{I_i} = 3$. An overdamped transient response to the step input is expected for this design. The system is stable with $K_h K_{I_i} < 20$. A similar analysis can be done for roll and pitch task space coordinates.

6. EXPERIMENTAL RESULTS

The control scheme was tested on the 3DOF pneumatic parallel robot. The inner and the external loops are both implemented in a Pentium-D 3.00-GHz connected to the robot through a Humusoft MF624 board. The board reads the joint's positions from linear potentiometric sensors, executes the control algorithm and gives the control signal to the electro-pneumatic valves with a sampling period of 1 ms. The task space variables are acquired by the same card, reading an encoder for the height; and pitch and roll angles via IMU [15]. In this loop the inverse kinematic problem is solved and the obtained vector of joint's coordinates $\mathbf{q}_d$ is given as desired joint positions to the internal loops. The control algorithm has been implemented using MATLAB/Simulink with the Real-Time Windows Target.

As shown in Fig. 8 the control system has two loops, the internal loop is solving the joint's control (decoupled control) with enough level of robustness to attenuate the undesirable effects of dynamics interactions between actuators, whereas the external loop executes the tracking task space control.

The equation (12) is satisfied, where the dynamic of the internal loop is dominated by a pair of conjugated complex poles (see section 4.1.), with 60 ms of sampling period for the external loop. A similar performance is obtained if the sampling period is 30 ms and the condition (12) is modified as $\mathbf{q}(k) = \mathbf{q}_d(k-2) \quad \forall k > 0$.

Figure 10 shows the joint's displacements during pulse train input signal with constant amplitude and frequency, where zero steady state error and the expected robustness of the closed-loop system against dynamic interactions between actuators are both achieved. Nevertheless, relatively large positioning errors appears in the cartesian coordinates from only implementation of decoupled position control scheme (see Fig. 11). Consequently, the moving platform pose can not be efficiently controlled only by the decoupled joint control.

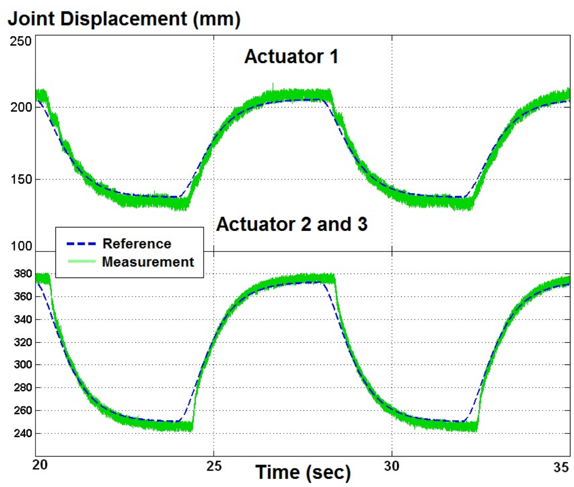

Fig 10: Results of experiments in joint positioning with decoupled position control

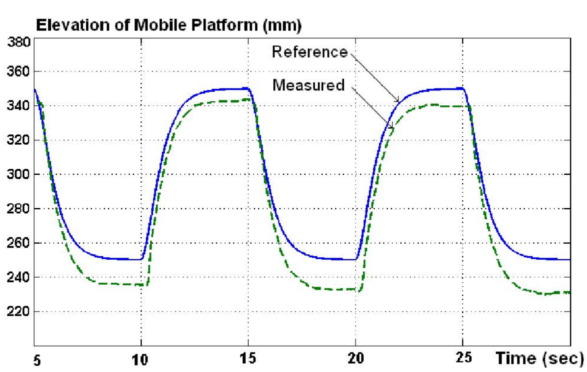

Fig 11: Cartesian errors in height positioning of end-effector

For that reason a cascade control scheme is then implemented for motion control purposes, by taking the advantages of two cascaded control loops architecture in task space configuration.

In the Fig. 12 is presented the platform task space output to simultaneous sine input in, θ_d, φ_d and h_d, demonstrating the good positioning performance, under the cascaded kinematics control scheme.

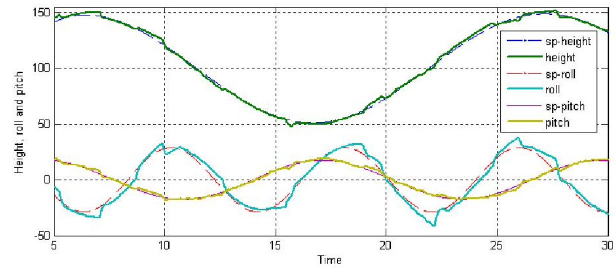

Fig 12: Task space control with sine input in: θ_d, φ_d and h_d without positioning errors of mobile platform

7. CONCLUSION

In this work a kinematic task space control scheme is implemented in a 3DOF pneumatic parallel industrial robot, based on the two cascaded loops control scheme and exteroceptive pose measurement. The internal loop solving the robot's joint control and the external loop is implementing as the task space control. The improvement of the performance of the control system is demonstrated with the kinematic task space control scheme, in relation with the joint control scheme. The experimental results confirm the expected performance of the system in the task space configuration. The two loops architecture gives flexibility to simulate and implement many robot's control strategies by modifying the outer loop control, while leaving the inner loop unchanged. On the other hand, the exteroceptive measuring system provide achievable dynamic positional and orientation accuracy in the range of control frequencies, taking as feasible end-effector pose measurement solution for the SIMPRO 3-DOF pneumatic parallel robot. Control algorithms are relatively simple and consequently feasible to implement in real-time industrial application, where fine positioning control and excellent stability are both achieved. Future researches will be addressed to improve the overall performance of the system under dynamic load uncertainties, external disturbance forces and noise measurements.

REFERENCES

[1] Merlet, J. P. *Parallel Robots*, 2nd Edition, Springer, France, 2006.

[2] Wang, H. and Xie, Y. "Adaptive Jacobian Position/force Tracking Control of Free-flying Manipulators," *Robotics and Autonomous Systems,* vol. 57, no. 2, pp. 173-181, 2009.

[3] Zhao, D., Li, S., Zhu, Q. "A new TSMC prototype robust nonlinear task space control of a 6 DOF parallel robotic manipulator," *International Journal of Control, Automation, and Systems,* vol. 8, no. 6, pp. 1189-1197, December 2010.

[4] Gao, J., Webb, P. and Gindy, N. "Evaluation of-Gao a Low-cost Inertial Dynamic Measurement Sys-

tem," *IEEE Conference on Robotics, Automation and Mechatronics,* Chengdu, China, pp. 1-5, 2008.

[5] Sokolov, A. and Xirouchakis, P. "Dynamics Analysis of a 3-DOF Parallel Manipulator with RPS Joint Structure," *Mechanism and Machine Theory,* vol. 42, no. 2, pp. 541-557, 2007.

[6] Xu, Q. and Li, Y. "Dynamic Modeling and Robust Control of a 3-PRC Translational Parallel Kinematic Machine," *Robotics and Computer-Integrated Manufacturing,* vol. 25, no. 3, pp. 630-640, 2009.

[7] Paccot, F. , Andreff, N., Martinet, P. and Khalil, W. "A Vision-based Computed Torque Control for Parallel Robots," *IEEE International Conference on Robotics and Automation,* Pasadena, USA, pp. 351-358, 2008.

[8] Kim, H. S., Cho, Y. M., Lee, K. "Robust Nonlinear Task Space Control for 6 DOF Parallel Manipulator," *Automatica,* vol. 41, pp. 1591-1600, June 2005.

[9] Qi, Z., Mcinroy, J. E. , Jafari, F. "Trajectory Tracking with Parallel Robots Using Low Chattering, Fuzzy Sliding Mode Controller," *Journal of Intelligent and Robotic Systems,* vol. 48, no. 3, pp. 333-356, March 2007.

[10] Hernández, L., Izaguirre, E., Rubio, E. and Urquijo, O. "Kinematic task space control scheme for 3DOF pneumatic parallel robot," *InTech, Intelligent Mechatronics,* Vienna, Austria, pp.67-84, 2011.

[11] Rubio, E. "Modelación, identificación y control de actuadores electro-neumáticos para aplicaciones industriales," *Ph.D. Thesis, Universidad Central Marta Abreu de Las Villas,*, 2009.

[12] Izaguirre, E., Hernández, L., Rubio, E., Prieto, P.J., Hernández, A. "Control Desacoplado de Plataforma Neumática de 3-gdl utilizada como Simulador de Movimiento," *Revista Iberoamericana de Automática e Informática Industrial,* vol. 8, no. 4, pp. 345-356, 2011.

[13] Izaguirre, E. "Task Space Kinematics Control of Pneumatic Parallel Robot in Motion Simulator Application," *Ph.D. Thesis, Universidad Central Marta Abreu de Las Villas*, 2012.

[14] Faugere, J-C. , Merlet, J-P and Rouillier, F. "On Solving the Direct Kinematics Problem for Parallel Robots," *Research Report, No. 5923, INRIA,* Institut National de Recherche en Informatique et en Automatique, Sophia-Antipolis, France, pp. 1-21, 2006.

[15] Izaguirre, E., Hernández, L., Rubio, E. and Urquijo, O. "Cartesian Control of a 3-DOF Electropneumatic Actuated Motion Platform with Exteroceptive Pose Measurement," *International Journal of Advanced Robotic Systems,* vol. 8, no. 4, pp. 120-128, 2011.

[16] Bonfe, M., Minardi, E. and Fantuzzi, C. "Variable Structure PID Based Visual Servoing for Robotic Tracking and Manipulation," *International Conference on Intelligent Robots and Systems,* Lausanne, Switzerland, pp. 396-401, October 2002.

Eduardo Izaguirre received the Ph.D. degree in technical science from UCLV, Cuba, in 2012. He is currently a professor with the Dept. of Automatic Control and member of the GARP Research Group. His current research interests include kinematics and dynamics modeling, simulation and control of industrial parallel robots.

Luis Hernández received the Ph.D. degree in technical science from Universidad Central Marta Abreu de Las Villas -UCLV-, Cuba, in 1994. He is currently a professor with the Dept. of Automatic Control and leader of the Research Group of Automatic, Robotics and Perception -GARP-. His research interests are focused on automatic control, autonomous vehicles and robotics.

Orlando Urquijo received the B.S. degree in automatic control from UCLV, Cuba, in 2009. He is currently a lecturer with the Dept. of Automatic Control and member of the GARP Research Group. His current research include kinematics modeling, simulation and control of motion simulators.